GEOPHYSICS, VOL. 67, NO. 6 (NOVEMBER-DECEMBER 2002); P. 1877–1885, 8 FIGS.
10.1190/1.1527087

Downloaded 09/15/14 to 86.134.248.35. Redistribution subject to SEG license or copyright; see Terms of Use at http://library.seg.org/

Simultaneous inversion of prestack seismic data for rock properties using simulated annealing

Xin-Quan Ma*

ABSTRACT

A new prestack inversion algorithm has been developed to simultaneously estimate acoustic and shear impedances from P-wave reflection seismic data. The algorithm uses a global optimization procedure in the form of simulated annealing. The goal of optimization is to find a global minimum of the objective function, which includes the misfit between synthetic and observed prestack seismic data. During the iterative inversion process, the acoustic and shear impedance models are randomly perturbed, and the synthetic seismic data are calculated and compared with the observed seismic data. To increase stability, constraints have been built into the inversion algorithm, using the low-frequency impedance and background V_s/V_p models. The inversion method has been successfully applied to synthetic and field data examples to produce acoustic and shear impedances comparable to log data of similar bandwidth. The estimated acoustic and shear impedances can be combined to derive other elastic parameters, which may be used for identifying of lithology and fluid content of reservoirs.

INTRODUCTION

In the last decade or so, there has been increased interest in prestack inversion because prestack inversion can be used to extract both compression and shear information from P-wave data acquisition (Goodway et al., 1997; Gray and Anderson, 2000). The shear wave information is contained in the variation of reflection coefficients with source-receiver offset (AVO). To detect the fluid content within reservoirs, both P- and S-wave properties of a rock are required because P-waves are sensitive to changes in pore fluid, whereas S-waves mainly interact with the rock matrix, relatively unaffected by the pore fluid. Prestack inversion can be useful in direct hydrocarbon indicators for both clastic and carbonate rocks, and it can be significant for lithology and fluid discrimination (Goodway et al., 1997; Burianyk, 2000; Gray and Andersen, 2000).

Prestack inversion for rock properties has been addressed by many workers in the past using a generalized linear inversion (GLI) technique (Tarantola, 1986; Mora, 1987; Demirbag et al., 1993; Pan et al., 1994). The GLI is an iterative process, requiring derivative information of an objective function and a good starting model for the effective optimization of model parameters. In the last decade, prestack inversion has also been attempted using global optimization algorithms such as genetic algorithm (GA) and simulated annealing (SA) (Sen and Stoffa, 1991; Mallick, 1995). GA is a statistical optimization technique using a natural analogy to biological evolution, whereas SA is analogous to the chemical process of crystal growing in a melt. Both algorithms belong to a directed Monte-Carlo approach, and have advantages over the GLI method in that they can effectively find a global minimum regardless of the shape of an objective function and independent of starting models (Goffe et al., 1994).

A recent approach to estimating P-wave and S-wave rock properties from prestack seismic data involves two separate stages (Goodway et al., 1997; Ma, 2001b). The first stage is to derive normal incidence P- and S-wave reflectivities through the AVO analysis (Fatti et al., 1994). The second stage is to apply an inversion algorithm to the AVO-derived reflectivity series, converting them into acoustic and shear impedances. Ma (2001b) developed a joint inversion technique which simultaneously estimates acoustic and shear impedances from the AVO-derived P- and S-wave reflectivity data. He used the SA algorithm to optimize a multivariable objective function and allowed multiple constraints to be built into the inversion scheme for efficiency and stability.

In this paper, I extend Ma's (2001b) joint inversion technique to simultaneously invert for rock properties from prestack P-wave offset seismic gathers. I combine the AVO extraction and impedance inversion into a single step, and formulate it as an global optimization problem. This means that, to transform P-wave offset seismic-reflection data into rock properties, there is no need to perform the AVO analysis for the estimates

Manuscript received by the Editor December 27, 2000; revised manuscript received April 11, 2002.
*Formerly Scott Pickford Group Limited, Leon House, 233 High Street, Croydon CR0 9XT United Kingdom; presently CGG Borehole, Ravensbourne, Westerham Road, Keston, Kent BR2 6HE, United Kingdom. E-mail: xqma@cgg.com.
© 2002 Society of Exploration Geophysicists. All rights reserved.

Downloaded 09/15/14 to 86.134.248.35. Redistribution subject to SEG license or copyright; see Terms of Use at http://library.seg.org/

of P- and S-wave reflectivities. The optimization procedure also adapts the SA algorithm, allowing flexible constraints to be built in. The outputs of the simultaneous inversion are acoustic and shear impedances. Both synthetic and field data examples are shown to demonstrate the validity of this new technique.

A SIMULTANEOUS INVERSION SCHEME

The Zoeppritz equations describe the relations of incident, reflected, and transmitted longitudinal waves and shear waves on both sides of a plane interface. The Aki and Richards (1980) equation gives an approximate relationship between the P-wave reflection coefficient $R(\theta)$ and the angle of incidence θ:

$$R(\theta) \approx \frac{1}{2}\left(\frac{\Delta V_p}{V_p} + \frac{\Delta\rho}{\rho}\right) - 2\left(\frac{V_s}{V_p}\right)^2\left(2\frac{\Delta V_s}{V_s} + \frac{\Delta\rho}{\rho}\right) \times \sin^2\theta + \frac{1}{2}\frac{\Delta V_p}{V_p}\tan^2\theta, \quad (1)$$

where V_p is the average P-wave velocity between two uniform half-spaces, V_s is the average S-wave velocity, and ρ is the average density. The assumptions made are that the relative changes of property ($\Delta V_p/V_p$, $\Delta V_s/V_s$, and $\Delta\rho/\rho$) are small, that the second-order terms can be neglected, and that θ is much less than 90°. Equation (1) can be rewritten in terms of P-wave and S-wave impedances:

$$R(\theta) \approx (1+\tan^2\theta)\frac{\Delta I_p}{2I_p} - 8\left(\frac{V_s}{V_p}\right)^2\sin^2\theta\frac{\Delta I_s}{2I_s} - \left[\tan^2\theta - 4\left(\frac{V_s}{V_p}\right)^2\sin^2\theta\right]\frac{\Delta\rho}{2\rho}, \quad (2)$$

where $I_p = V_p\rho$ is the average acoustic impedance, $I_s = V_s\rho$ is the average shear impedance, $\Delta I_p/2I_p = 1/2(\Delta V_p/V_p + \Delta\rho/\rho)$ is the zero-offset P-wave reflection coefficient, and $\Delta I_s/2I_s = 1/2(\Delta V_s/V_s + \Delta\rho/\rho)$ is the zero-offset S-wave reflection coefficient. It can be shown that the third term in ρ only cancels for most V_s/V_p ratios around 0.5 and small angles (Fatti et al., 1994). Equation (2) then simplifies to

$$R(\theta) \approx (1+\tan^2\theta)\frac{\Delta I_p}{2I_p} - 8\left(\frac{V_s}{V_p}\right)^2\sin^2\theta\frac{\Delta I_s}{2I_s}. \quad (3)$$

The equation (3) has been used by Fatti et al. (1994), Goodway et al. (1997), and Ma (2001b) to extract P- and S-wave impedance reflectivities by fitting it to the P-wave reflection amplitudes from real common-midpoint (CMP) gathers. However, the background V_s/V_p ratio must be known a priori. If the background V_p and V_s models are not a good approximation of an earth model, the linear AVO inversion for reflectivity could produce a biased and physically unreasonable solution (Wang, 1999). To overcome this limitation, I replace the average V_s/V_p ratio by the average I_s/I_p ratio, so that the reflection coefficients $R(\theta)$ are only related to three parameters: I_p, I_s, and θ. Among those, the angle of incidence θ can be calculated using a ray-tracing method (Smith and Gidlow, 1987). This substitution is valid when the density change between two adjacent layers is small. Note that the average I_s/I_p is not determined from background P- and S-impedance models, but it is derived from the impedance models at each iteration. Equation (3) is now rearranged as

$$R(\theta) \approx (1+\tan^2\theta)\frac{\Delta I_p}{2I_p} - 8\left(\frac{I_s}{I_p}\right)^2\sin^2\theta\frac{\Delta I_s}{2I_s}. \quad (4)$$

Based on equation (4), I propose a simultaneous inversion procedure to estimating acoustic and shear impedances from prestack offset seismic gathers. The basic assumptions made are that the earth has approximately horizontal layers at each common depth point, and that each layer is described by both acoustic and shear impedances. The simultaneous inversion is achieved by using the Monte-Carlo approach in the form of simulated annealing. A solution vector to be optimized comprises n acoustic impedance values followed by n shear impedance values, where n is the number of layers. From a given starting model, zero-offset P- and S-impedance reflection coefficients at an interface i can be calculated as

$$\frac{\Delta I_p}{2I_p} = \frac{I_p^i - I_p^{i-1}}{I_p^i + I_p^{i-1}}, \qquad \frac{\Delta I_s}{2I_s} = \frac{I_s^i - I_s^{i-1}}{I_s^i + I_s^{i-1}}, \quad (5)$$

and the average Is/Ip ratio between layer $i-1$ and layer i can also be calculated as

$$\frac{I_s}{I_p} = \frac{I_s^i + I_s^{i-1}}{I_p^i + I_p^{i-1}}. \quad (6)$$

By substituting equations (5) and (6) into equation (4), one can calculate reflection coefficients $R(\theta)$ for each offset and at each layer boundary for an earth model prescribed by impedances I_p^i and I_s^i. A synthetic offset seismic gather can be calculated by convolving the reflection coefficients $R(\theta)$ with predetermined wavelets. These synthetic data are compared with the observed data to form a misfit function. We then randomly perturb each parameter of the solution vector in turn to form a new earth model, and generate new synthetic data, which are compared with the observation again. The process is repeated until a sufficient agreement between the observed and the synthetic data is achieved. The above procedure can be described within an optimization framework (i.e., one needs to find a global minimum of a multivariable objective function by means of simulated annealing). Once the global minimum is found, the corresponding model parameters are the resultant earth model. To reduce the nonuniqueness problem, the inversion algorithm is constrained by low-frequency macromodels, which may be obtained from seismic stacking velocities or from log information.

SIMULATED ANNEALING

SA is a global optimization technique that is analogous to the natural process of crystal annealing when a liquid gradually cools to a solid state. The SA technique starts with an initial model $\mathbf{m}_0$, with associated energy or misfit $f(\mathbf{m}_0)$. It draws a new model $\mathbf{m}_\mathbf{n}$. The associated misfit $f(\mathbf{m}_\mathbf{n})$ is then computed and compared against $f(\mathbf{m}_0)$. If the misfit $f(\mathbf{m}_\mathbf{n})$ is

Downloaded 09/15/14 to 86.134.248.35. Redistribution subject to SEG license or copyright; see Terms of Use at http://library.seg.org/

lower than that of the starting model, the new model is accepted unconditionally. However, if it is larger than that of the starting model, then the new model is accepted with the probability $p = \exp[-(f(\mathbf{m_n}) - f(\mathbf{m}_0)/T]$, where T is a control parameter called the acceptance temperature. This acceptance rule is known as the Metropolis criterion (Metropolis et al., 1953). The same process is repeated a large number of times, with the annealing temperature gradually decreasing according to a cooling schedule. The algorithm is stopped when the misfit does not change after a sufficient number of trials. Since the probability of accepting a model in an uphill direction is always greater than zero, the algorithm can climb out of a local minimum. A more detailed description of the SA algorithm can be found in Goffe et al. (1994) and Ma (2001a).

OBJECTIVE FUNCTION

In this paper, I use an L_1-norm error function for the objective function. This is the least absolute deviation between the observed and modeled offset seismic gather. In order to constrain the impedance models, I add a priori impedance and a priori I_s/I_p misfits. These constraints guide the solution towards the low frequency impedance (I_s, I_p) and I_s/I_p ($=V_s/V_p$) trends. The objective function is expressed as

$$\Delta f = W_1 \frac{\sum_{j=1}^{m}\sum_{i=1}^{n}\left|S_{\text{obs}}^{ij} - S_{\text{mod}}^{ij}\right|}{\sum_{j=1}^{m}\sum_{i=1}^{n}\left|S_{\text{obs}}^{ij}\right|} + W_2\left(\frac{\sum_{i=1}^{n}\left|I_{p\text{pri}}^{i} - I_{p\text{mod}}^{i}\right|}{\sum_{i=1}^{n}\left|I_{p\text{pri}}^{i}\right|} + \frac{\sum_{i=1}^{n}\left|I_{s\text{pri}}^{i} - I_{s\text{mod}}^{i}\right|}{\sum_{i=1}^{n}\left|I_{s\text{pri}}^{i}\right|}\right) + W_3\frac{\sum_{i=1}^{n}\left|\frac{I_{s\text{pri}}^{i}}{I_{p\text{pri}}^{i}} - \frac{I_{s\text{mod}}^{i}}{I_{p\text{mod}}^{i}}\right|}{\sum_{i=1}^{n}\left|\frac{I_{s\text{pri}}^{i}}{I_{p\text{pri}}^{i}}\right|}, \quad (7)$$

where S_{obs}^{ij} is the observed seismic amplitude at time index i and channel index j, S_{mod}^{ij} is the synthetic seismic amplitude at time index i and channel index j, $I_{p\text{pri}}^{i}$ is an a priori low-frequency P-impedance trend at time index i, $I_{p\text{mod}}^{i}$ is the modeled P-impedance at time index i, $I_{s\text{pri}}^{i}$ is an a priori low frequency S-impedance trend at time index i, $I_{s\text{mod}}^{i}$ is the modeled S-impedance at time index i, n is the number of samples in a seismic trace, m is the number of channels in a seismic gather, and W_1, W_2, and W_3 are weights applied to the three terms, respectively.

Note that while the number of terms summed in the first component of the objective function is $m \times n$, the exact number of parameters to be solved by the global optimisation is $2n$. A parameter vector consists of n P-impedance samples followed by n S-impedance samples. This is a fine-layered parameterization of an earth model in which only impedances need to be solved. Before inversion, seismic amplitudes have to be scaled to the level such that they match a synthetic gather generated from well log data. Three logs (V_p, V_s, and ρ) allow us to generate offset-dependant reflection coefficients using either the Zoeppritz equations or Aki and Richard's (1980) approximation [equation (1)], in which the angle of incidence θ is determined by ray tracing. A synthetic seismic gather is then generated by convolving the synthetic reflection coefficients with a wavelet estimated from the real seismic data. A scaling factor can be found by matching the amplitudes of the real data to that of the synthetic data, and is applied to the real data before inversion. Since the three terms in the objective function have been normalized, the weighting factors can be chosen as $W_1 = W_2 = W_3 = 1$ in most cases. These weights are used in both synthetic and field examples presented later in this paper.

FORWARD MODELING

To calculate the objective function, one needs to model synthetic seismic responses. Although the finite difference of a 3-D wave equation (Reshef et al., 1988) may be used, the computation is too intensive to be practical for seismic inversion in which many thousands of iterations are needed. The reflectivity method (Kennett, 1983) requires seismic data to be converted from the time-distance domain into the frequency-wavenumber domain. When the number of recording channels is limited, aliasing may affect the quality of inversion.

In this paper, I use a convolutional model to generate synthetic data. It is assumed that in laterally homogeneous acoustic media, prestack seismic data can be approximated by convolution of offset-dependent reflection coefficients with a known wavelet. The convolutional model assumes plane-wave propagation across the boundaries of horizontally homogeneous layers, and takes no account of the effects of geometrical divergence, anelastic absorption, wavelet dispersion, transmission losses, mode conversions, and multiple reflections. For a convolution model to be valid, the seismic data must be processed to eliminate those effects and to restore plane-wave amplitudes of primary P-wave reflections.

The seismic source wavelet can be estimated using various techniques (White, 1980). For prestack inversion, seismic wavelets must be determined to compensate for offset-dependent phase, bandwidth, tuning, and NMO stretch effects. These wavelets can be estimated by shaping between modeled logs and multioffset stacks (Pendrel et al., 2000).

CONSTRAINTS FOR INVERSION

The impedance solution from seismic inversion is nonunique outside the bandwidth of the source wavelet. Very low frequency information about acoustic impedance is not directly derivable from band-limited seismic data. Without constraints, there may be many solutions with different low-frequency trends all equally satisfying the observation. The inversion process also rejects any frequencies higher than the wavelet bandwidth. Any number of thin layers can be added to the acoustic impedance profile without significantly affecting the fit to the data. Without appropriate constraints, the solution may exhibit strong, unstable oscillations and show a poor match between the true and estimated impedances.

To reduce the nonuniqueness and stabilize the solution, I apply the following constraints to the algorithm:

1) A priori acoustic and shear impedance information, derived from well log and NMO velocity, is used as

Downloaded 09/15/14 to 86.134.248.35. Redistribution subject to SEG license or copyright; see Terms of Use at http://library.seg.org/

a constraint in the objective function [see term 2 in equation (7)]. This term guides the solution towards the physically meaningful low-frequency trend. An a priori I_s/I_p constraint is also added to guide the search to follow the background I_s/I_p trend. With these constraints in place, the impedance solution will contain the low-frequency component, which is missing from band-limited seismic data.

2) A search boundary is set up for each parameter, limiting the physical properties such that the set of possible solutions exists only within a defined corridor. The parameter bounds are derived directly from the low-frequency impedance trend. Both P-impedance and S-impedance boundaries are set up to constrain the $2n$ model parameters. A good selection of parameter bounds reduces the nonuniqueness problem and also minimises the computing time. However the bounds must be chosen wide enough for true impedance models to exist within the defined corridors. In practice, corridor widths of 6000 m/s × g/cm^3 and 4000 m/s × g/cm^3 are used for P-impedance and S-impedance, respectively.
3) The search boundary is further modified by seismic amplitudes. This is based on the fact that layer boundaries with large impedance contrasts exhibit large amplitudes in seismic data. Therefore, one should allow a wider search corridor for interfaces at which seismic amplitudes are large, and a narrower corridor for places where seismic amplitudes are small. In practice, an rms gain

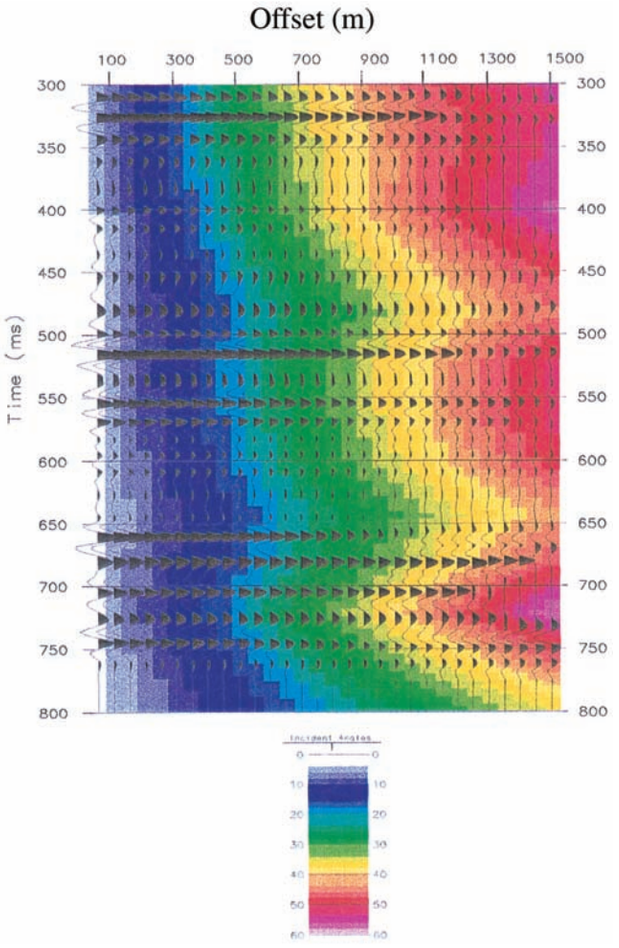

FIG. 1. A synthetic seismic gather superimposed over the angle of incidence. The angle range used for inversion is 0–40°.

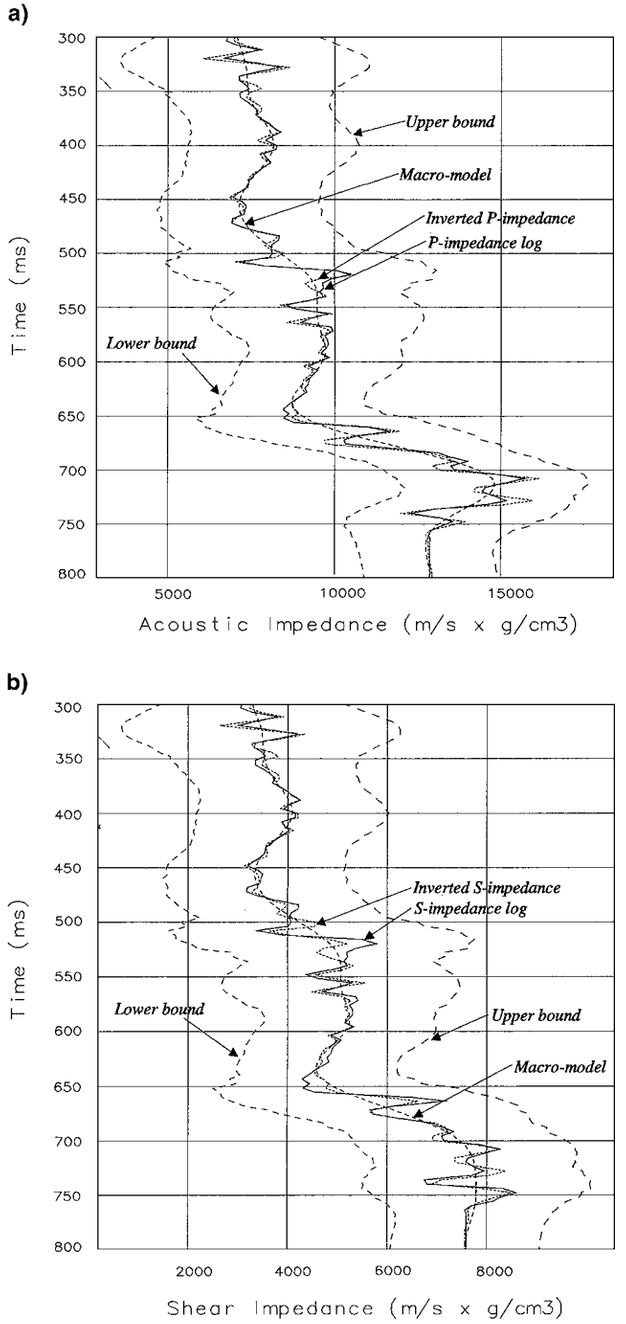

FIG. 2. Simultaneous inversion for acoustic (a) and shear (b) impedances from a synthetic seismic gather shown in Figure 1. The lower boundaries of P- and S-impedance models are defined by subtracting 3000 m/s × g/cm^3 from the macro P-impedance model and 2000 m/s × g/cm^3 from the macro S-impedance models, respectively. The upper boundaries are defined by adding those values into the macromodels. These boundaries are later modified by the use of seismic envelopes.

curve of a stacked seismic trace from a CMP gather is calculated and incorporated into the parameter search boundaries.

SYNTHETIC DATA EXAMPLE

One set of P-wave velocity V_p, S-wave velocity V_s, and density ρ logs completely defines the elastic properties of a horizontally layered and isotropic 1-D medium. I use these three logs to generate a synthetic seismic CMP gather. The offset-dependent reflection coefficients $R(\theta)$ are generated using exact Zoeppritz equations. Angles of incidence are estimated by 1-D ray tracing using P-wave velocity. A synthetic seismic gather is generated by convolving reflection coefficients $R(\theta)$ with a Ricker wavelet of a central frequency 60 Hz. The offset between traces is 50 m, and the maximum distance range is 1500 m. The synthetic data reveals clearly the amplitude variations with offsets (Figure 1).

Once the incident angles (θ) are generated, they are considered known and fixed during the stochastic inversion procedure. However, only a certain range of angles may be chosen for inversion. A mute in low angles eliminates the near-offset effect due to a low signal-to-noise ratio, and a mute in high angles reduces the far-offset distortion due to the NMO stretch. In this synthetic example, the angle range is chosen as 0–40°.

The simultaneous inversion procedure begins by calculating the objective function using the initial model parameters. A starting model can be drawn from either a random model or a macromodel. A new model is accepted or rejected according to the Metropolis criteria (Metropolis et al., 1953). At a given temperature, many iterations are performed. The temperature is then lowered until the convergence criterion is eventually satisfied. The outputs are the optimized acoustic and shear impedance values at each sample interval. Since the average V_s/V_p ratio in equation (3) has been replaced by the I_s/I_p ratio, which is also perturbed with impedance models, there are no a priori restrictions on the magnitude of I_s/I_p; a constant V_s/V_p, or the one derived from low frequency V_s and V_p models, could produce a biased solution (Wang 1999). Tests have shown that drawing the average V_s/V_p from impedance models can also speed up the convergence and therefore make the computation more efficient.

Estimated acoustic and shear impedances are shown in Figures 2a and 2b, respectively. It can be seen that the parameter search corridor follows the trend of the macromodel, with localized variations introduced by seismic envelopes. The search boundaries are defined differently for acoustic impedance and shear impedance profiles. The estimated P- and S-impedances match well with their true models. As an additional quality control, a synthetic seismic gather is reconstructed (Figure 3) using the inverted impedances and plotted along with the synthetic seismic gather of Figure 1. They indicate that the residual energy (misfit) is very small. Meanwhile, the synthetic gather for the starting model is also calculated and displayed following the input synthetic gather. It can be seen that the initial gather has nothing in common with the input gather because the starting impedance model is randomly generated.

FIELD DATA EXAMPLE

The prestack seismic data are from a North Sea 3-D survey. The key ingredients in the processing sequence include predictive deconvolution, offset variant gain recovery, Radon multiple attenuation, and prestack 3-D time migration. The gathers were NMO corrected. The seismic CMP gather near a well location, superimposed on to the gather of incident angle, is shown in Figure 4.

There are three wells in the area for which the P-wave velocity and density logs are available. S-wave velocity was derived from an empirical relationship between V_s and V_p obtained

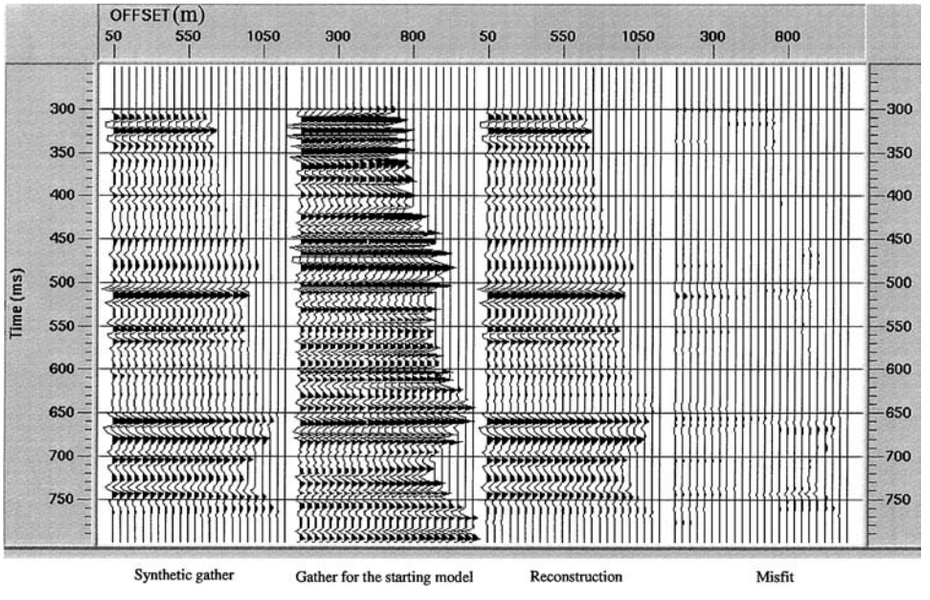

FIG. 3. Comparison of the synthetic seismic gather shown in Figure 1 with the reconstruction using inverted impedances shown in Figure 2. The misfit gather shows the differences between the synthetic and reconstructed gathers. Also shown is the seismic gather for the starting model, which is randomly generated.

Downloaded 09/15/14 to 86.134.248.35. Redistribution subject to SEG license or copyright; see Terms of Use at http://library.seg.org/

from nearby wells outside this survey area. These logs and interpreted seismic horizons were used to construct macro-velocity and impedance models. Three wavelets were derived using a partial coherence method (White, 1980) at the wells. The wavelets all had a similar dominant phase. The consensus

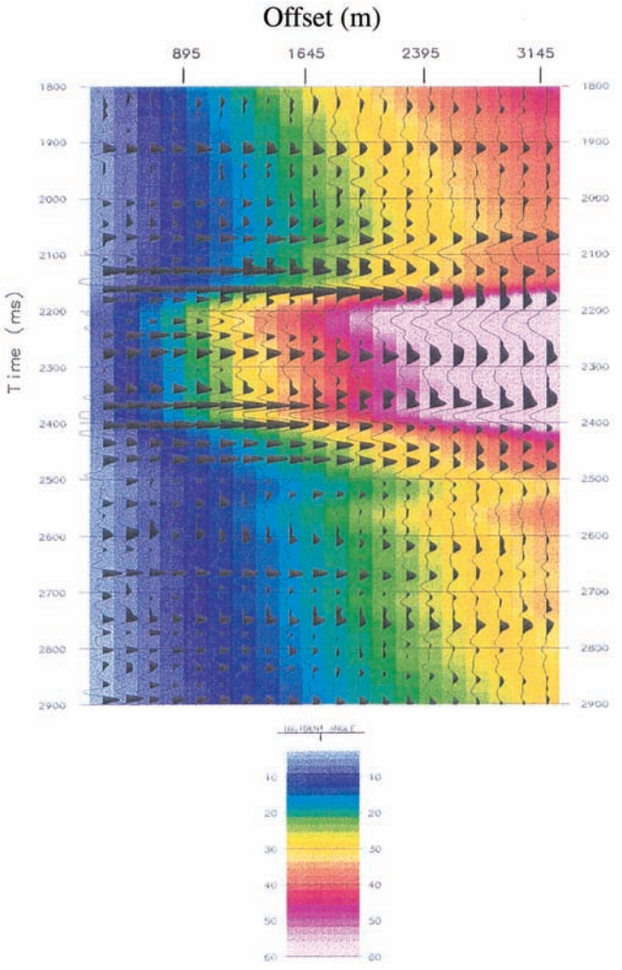

FIG. 4. A real seismic gather from a North Sea 3-D survey. The angle of incidence is determined by 1-D ray tracing using macro P-wave velocity. The angle range used for inversion is 0–40°.

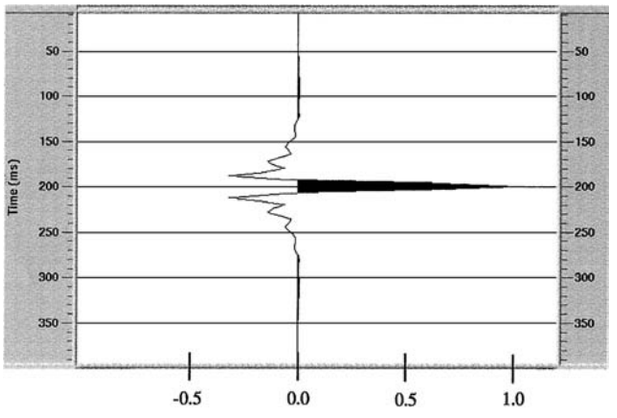

FIG. 5. A zero-phase wavelet, estimated using three well locations, is used for forward modeling.

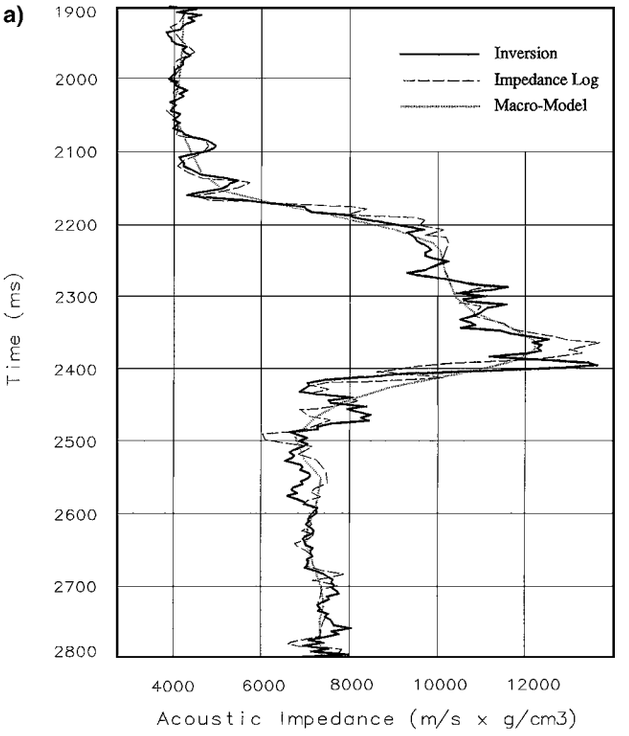

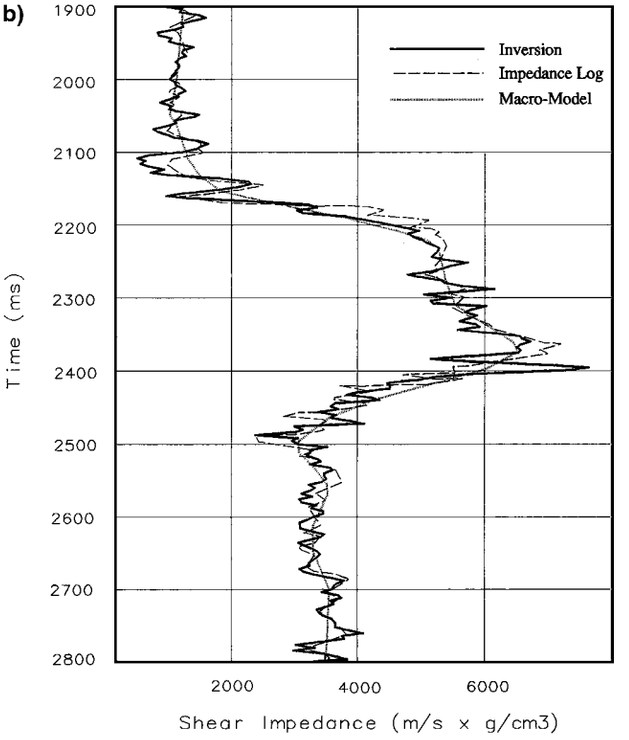

FIG. 6. Simultaneous inversion for acoustic (a) and shear (b) impedances from a real seismic gather shown in Figure 4. Macro impedance models are used to constrain the inversion through the two misfit terms defined in the objective function, and also to set up parameter search boundaries (not shown).

Downloaded 09/15/14 to 86.134.248.35. Redistribution subject to SEG license or copyright; see Terms of Use at http://library.seg.org/

Downloaded 09/15/14 to 86.134.248.35. Redistribution subject to SEG license or copyright; see Terms of Use at http://library.seg.org/

wavelet I finally used combines the averaged dominant phase with the bandwidth of the data. Since the signal is changing only little with offset in the target window, the single consensus wavelet was used for the prestack inversion (Figure 5). The NMO-corrected CMP gather and low-frequency P-wave velocity and acoustic and shear impedances were the inputs to the inversion. Again, the parameter search boundaries were constructed from macromodels and subsequently modified by seismic amplitude envelopes. The inversion is constrained at each time sample by the low-frequency P- and S-impedances and I_s/I_p ratios. The outputs from the inversion are the estimated acoustic and shear impedances and their misfits, measured by the objective function in equation (7). Figure 6 shows a comparison between the inverted and log impedances, revealing that the match is reasonably good. Figure 7 shows the reconstruction of a seismic gather near the well location using the resultant impedance solution and the same angle of incidence as used in inversion. It can be seen that the reconstruction matches the input gather very well. The misfit (residual energy) is believed to be noise in seismic data. A synthetic gather for the starting model shows much smaller amplitudes because a smooth macro impedance model is taken as the starting model. Figures 8a and 8b show the results for a seismic inline crossing one of the wells. The inverted P- and S-impedances show very high vertical resolution and lateral consistency. For comparison purposes, I insert acoustic and shear impedance logs at the well location, both showing quite good matches. The inverted impedances allow for improved reservoir characterisation.

ROCK PROPERTIES DERIVED FROM P- AND S-IMPEDANCES

Reservoir characterization requires the detection, identification, and quantification of thickness, porosity, permeability, and fluid content. Unfortunately, many of these reservoir parameters are not directly derivable from seismic data. Only a few elastic parameters such as Lamé's constants, velocities, Poisson's ratio, and impedances are directly responsible for seismic amplitude variation, and are therefore derivable from seismic data. Experimental and empirical relationships between elastic parameters and rock properties enable us to characterize reservoirs using seismic data combined with petrophysical observations.

Acoustic and shear impedances estimated using the simultaneous inversion scheme can be used to derive the conventional rock properties such as V_s/V_p or Poisson's ratio (σ). These properties can then be used to evaluate the lithology and pore fluid variations by means of crossplotting or statistical techniques (Ostrander 1984; Castagna et al., 1993). More recently, Goodway et al. (1997) introduced a technique of using elastic parameter λ (Lamé's constant) and μ (shear rigidity modulus) to discriminate gas sand from shales. This approach is based on the premise that λ values contain all the fluid information and approximately represent incompressibility, whereas μ is the rigidity of the rock matrix. Goodway's $\lambda\rho$ and $\mu\rho$ are directly derivable from acoustic and shear impedances by $\lambda\rho = I_p^2 - 2I_s^2$ and $\mu\rho = I_s^2$. Crossplotting $\lambda\rho$ versus $\mu\rho$ or $\lambda\rho$ versus λ/μ enables fluid content and lithology to be discriminated. This approach has been shown to be better hydrocarbon indicators than the conventional method using P- and S-velocities or P- and S-impedances (Goodway et al., 1997; Burianyk, 2000; Gray and Andersen, 2000).

CONCLUSIONS

The simultaneous inversion algorithm described in this paper combines the AVO extraction and impedance inversion into a single step, and transforms P-wave offset seismic gathers into

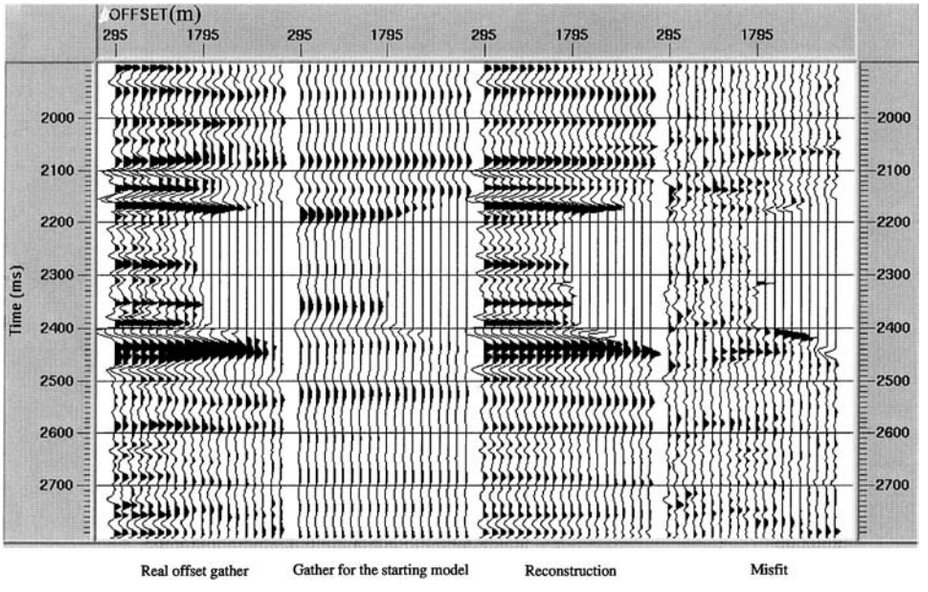

FIG. 7. Comparison of a real seismic gather shown in Figure 4 with the synthetic gather constructed using the inverted impedances shown in Figure 6. The misfit gather shows the differences between the real and synthetic gathers. Also shown is the synthetic gather for the starting model, which is taken from the macro impedance models.

P- and S-impedances using simulated annealing. Impedances are directly responsible for seismic responses, and therefore are better resolved by inversion. In addition, the use of impedances, rather than reflection coefficients, as model parameters allows reliable and flexible constraints to be included on the inversion algorithm.

The inversion algorithm is constrained by the low-frequency impedance models and further by background V_s/V_p ratios to reduce the nonuniqueness problem and to achieve maximum stability. The inversion procedure using the global optimization approach allows a high resolution of P- and S-impedances to be extracted over typical

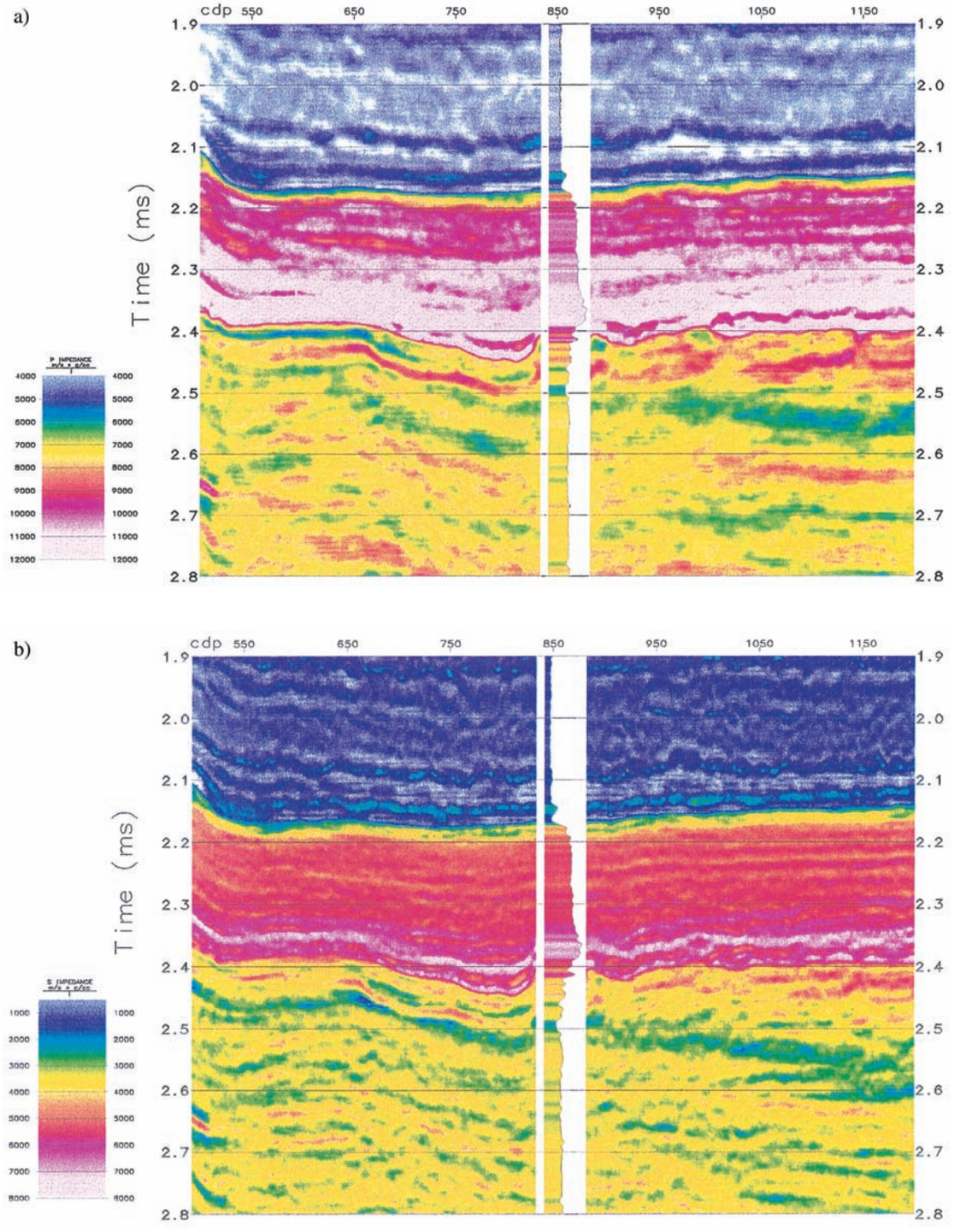

FIG. 8. Simultaneous inversion for acoustic (a) and shear (b) impedances from a North Sea 3-D survey. The inserts are the acoustic and shear impedance logs for comparison with the inversion results.

Downloaded 09/15/14 to 86.134.248.35. Redistribution subject to SEG license or copyright; see Terms of Use at http://library.seg.org/

reservoir intervals. It is therefore a suitable tool for reservoir characterization.

ACKNOWLEDGMENTS

The author thanks Paul Haskey of Scott Pickford Group for the stimulating discussions and proofreading this manuscript. The author also thanks Techmarine International Ltd. for providing the North Sea data.

REFERENCES

Aki, K., and Richards, P. G., 1980, Quantitative seismology: Theory and methods: W. H. Freeman and Co.

Burianyk, M., 2000, Amplitude-versus-offset and seismic rock property analysis: A primer: CSEG Recorder, **25**, No. 9, 6–16.

Castagna, J. P., Batzle, M. L., and Kan, T. K., 1993, Rock physics—The link between rock properties and AVO response, *in* Castagna, J. P., and Backus, M. M., Eds. Offset-dependent reflectivity—Theory and practice of AVO Analysis: Soc. Expl. Geophys., 135–171.

Demirbag, E., Coruh, C., and Costain, J. K., 1993, Inversion of P-wave AVO, *in* Offset-dependent reflectivity—Theory and practice of AVO Analysis: Soc. Expl. Geophys., 287–302.

Fatti, J. L., Smith, G. C., Vail, P. J., Strauss, P. J., and Levitt, P. R., 1994, Detection of gas in sandstone reservoirs using AVO analysis: A 3-D seismic case history using the Geostack technique: Geophysics, **59**, 1362–1376.

Goffe, W. L., Ferrier, G. D., and Rogers, J., 1994, Global optimisation of statistical functions with simulated annealing: J. Econometrics, **60**, 65–100.

Goodway, W., Chen, T., and Downton, J., 1997, Improved AVO fluid detection and lithology discrimination using Lame petrophysical parameters; "Lambda*Rho", "Mu*Rho" and "Lambda/Mu fluid stack", from P and S Inversions: Ann. Mtg., Can Soc. Expl. Geophys., Abstracts, 148–151.

Gray, D., and Andersen, E., 2000, Application of AVO and inversion to formation properties: World Oil, **221**, July, 85–90.

Kennett, B. L. N., 1983, Seismic wave propagation in stratified media: Cambridge Univ. Press.

Ma, X. Q., 2001a, A constrained global inversion method using an over-parameterised scheme: Application to poststack seismic data: Geophysics, **66**, 1–14.

———2001b, Global joint inversion for the estimation of acoustic and shear impedances from AVO derived P- and S-wave reflectivity data: First Break, **19**, 557–566.

Mallick, S., 1995, Model-based inversion of amplitude-variations with offset data using a genetic algorithm: Geophysics, **60**, 939–954.

Metropolis, N., Rosenbluth, A., Rosenbluth, M., Teller, A., and Teller, E., 1953, Equation of state calculations by fast computing machines: J. Chem. Phys., **21**, 1087–1092.

Mora, P., 1987, Non-linear two-dimensional elastic inversion of multi-offset seismic data: Geophysics, **52**, 1211–1228.

Ostrander, W. J., 1984, Plane wave reflection coefficients for gas sands at nonnormal angles of incidence: Geophysics, **49**, 1637–1648.

Pan, G. S., Young, C. Y., and Castagna, J. P., 1994, An integrated target-orientated prestack elastic waveform inversion: sensitivity, calibration, and application: Geophysics, **59**, 1392–1404.

Pendrel, J., Debeye, H., Pedersen-Tatalovic, R., Goodway, B., Dufour, J., Bogaards, M., and Stewart, R., 2000, Estimation and interpretation of P- and S-impedances from simultaneous inversion of P-wave offset seismic data, 70th Ann. Internat. Mtg: Soc. Expl. Geophys., Expanded Abstracts, 146–149.

Reshef, M., Kosloff, D., Edwards, M., and Hsiung, C., 1988, Three-dimensional elastic modeling by the Fourier method: Geophysics, **53**, 1184–1193.

Sen, M. K., and Stoffa, P. L., 1991, Nonlinear one-dimensional seismic waveform inversion using simulated annealing: Geophysics, **56**, 1624–1638.

Smith, G. C., and Gidlow, P. M., 1987, Weighted stacking for rock property estimation and detection of gas: Geophys. Prosp., **35**, 993–1014.

Tarantola, A., 1986, A strategy for nonlinear elastic inversion of seismic reflection data: Geophysics, **51**, 1893–1903.

Wang, Y., 1999, Simultaneous inversion for model geometry and elastic parameters: Geophysics, **64**, 182–190.

White, R. E., 1980, Partial coherence matching of synthetic seismograms with seismic traces: Geophys. Prosp., **28**, 333–358.

Downloaded 09/15/14 to 86.134.248.35. Redistribution subject to SEG license or copyright; see Terms of Use at http://library.seg.org/